Dynamic Changes in Schlemm Canal and Iridocorneal Angle Morphology During Accommodation in Children With Healthy Eyes: A Cross-Sectional Cohort Study

Moritz Claudius Daniel,[1,2] Adam M. Dubis,[1] Ana Quartilho,[1,3] Huda Al-Hayouti,[1] Sir Peng Tee Khaw,[1] Maria Theodorou,[1] and Annegret Dahlmann-Noor[1]

[1]National Institute for Health Research Biomedical Research Centre at Moorfields Eye Hospital NHS Foundation Trust and University College London Institute of Ophthalmology, London, United Kingdom
[2]Eye Center, Medical Center, University of Freiburg Faculty of Medicine, University of Freiburg, Freiburg, Germany
[3]Comprehensive Clinical Trials Unit, University College London, London, United Kingdom

Correspondence: Annegret Dahlmann-Noor, National Institute for Health Research Biomedical Research Centre at Moorfields Eye Hospital and UCL Institute of Ophthalmology, 162 City Road, London EC1V 2PD, UK; annegret.dahlmann-noor@moorfields.nhs.uk.

Submitted: October 19, 2017
Accepted: May 26, 2018

Citation: Daniel MC, Dubis AM, Quartilho A, et al. Dynamic changes in Schlemm canal and iridocorneal angle morphology during accommodation in children with healthy eyes: a cross-sectional cohort study. *Invest Ophthalmol Vis Sci*. 2018;59:3497–3502. https://doi.org/10.1167/iovs.17-23189

Purpose. The purpose of this study was to explore changes in Schlemm canal (SC), trabecular meshwork (TM), and iridocorneal angle (ICA) morphology during accommodative effort in children and young adults.

Methods. We acquired anterior segment optical coherence tomography images (AS-OCT) of the ICA and ciliary muscle (CM) of both eyes of 50 children age 4 to 16 years with healthy eyes, at two levels of accommodation: 2.5 and 15 diopters (D). Semiautomated nasal ICA measurements were as follows: angle opening distance at 500/750 μm (AOD-500, -750), trabecular iris space area at 500/750 μm (TISA-500, -750), and trabecular iris angle at 500/750 μm (TIA-500, -750). Manual measurements were as follows: anteroposterior and radial SC diameter (SC-APD, SC-RD), cross-sectional area of SC (SC-CSA) and TM height (TMH), TM length (TML), and TM density (TMD). CM width was measured at 1, 2, and 3 mm from the scleral spur (CM-1, CM-2, CM-3). For each parameter, a three-level random-effects model was fitted to estimate differences between the two levels of accommodation.

Results. With accommodative effort, SC diameters and CSA increase significantly, as do TM length and iridocorneal angle parameters. With increasing age, SC dimensions reduce. Angle parameters are smaller in eyes with greater spherical equivalent (hypermetropia).

Conclusions. AS-OCT can be used to visualize dynamic morphologic changes in outflow structures with physiologic accommodation. The increase in SC dimensions with accommodative effort may contribute to the regulation of IOP in children.

Keywords: aqueous flow, accommodation, ocular, humans

Little is known about the development of the iridocorneal angle (ICA) and the aqueous outflow structures during childhood and teenage years and about the possible link between developmental changes in amplitude of accommodation (AA) and IOP.

In the first few months after birth, mean IOP is approximately 8 to 10 mm Hg, increasing over the first years of life.[1–3] Evidence as to at which age IOP stabilizes or reaches adult values is conflicting, with figures varying between 4 and 12 years, with sex differences reported by some authors.[2–5] A gradual, linear decline in AA of around 1 diopter (D) per year from the age of 5 years until the late teens is, on the contrary, well described.[6–12] In children under the age of 11 years, there is a negative correlation between AA and IOP.[4] In young adults, sustained or repeated accommodative effort transiently lowers IOP.[13]

Histologic, pharmacologic, and electrophysiologic studies explain the link between accommodation and IOP: elastin fibers in the tendons of the longitudinal portion of the ciliary muscle (CM) connect to elastin fibers in the trabecular meshwork (TM) lamellae, with CM tendon fiber density greatest near the juxtacanalicular tissue, the part of the TM adjacent to Schlemm canal (SC).[14,15] CM contraction induced by pilocarpine or electrical stimulation of the Edinger Westphal nucleus stretches the TM and increases the cross-sectional area (CSA) of SC.[16–21] However, changes in SC and TM morphology with physiologic accommodation have not yet been demonstrated in humans.

Optical coherence tomography (OCT), particularly dedicated anterior segment OCT (AS-OCT), can visualize both SC and TM[22,23] and the anterior portion of the CM,[11,24,25] as well as provide automated measurements of ICA parameters.[26] The aim of the present study was to explore changes in SC, TM, and ICA morphology during accommodative effort in humans.

Methods

This cross-sectional cohort study was approved by the London–Stanmore Research Ethics Committee (16/LO/0327). The study adhered to the tenets of the Declaration of Helsinki. A research fellow (MD) screened the clinical records of children attending Moorfields Eye Hospital, London, UK, and invited eligible children and young people to take part.

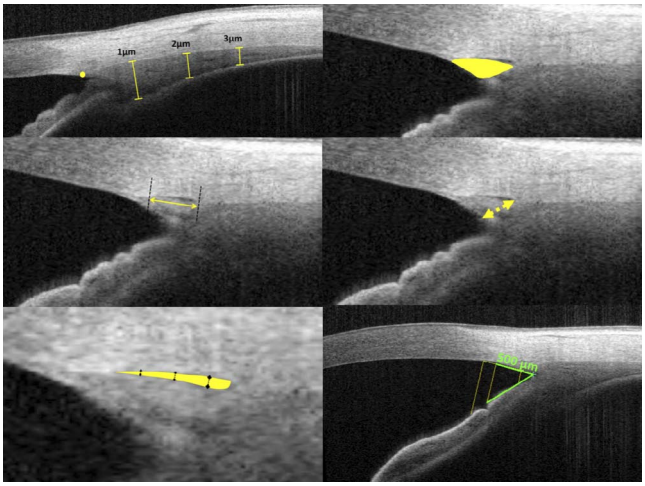

FIGURE. AS OCT measurements. *Left*, *top*: To confirm that accommodative effort was made, we measured ciliary muscle width at 1, 2, and 3 mm posterior to the scleral spur (CM1, 2, 3). CM1 is known to increase and CM3 to decrease with accommodation. *Center*: We defined the anteroposterior diameter of SC as the anteroposterior extent of the *black shape,* which represents SC on AS OCT. *Bottom*: As SC is frequently tear shaped, with greatest height posteriorly, we measured its radial diameter at three locations and calculated the average. We measured the SC-CSA by outlining the SC contour using the freehand tool and measuring the area of the resulting shape. *Right, top*: We defined the TM area as the area enclosed by a line connecting the scleral spur, posterior endpoint of SC, and Schwalbe's line. *Center*: We defined TM height as the distance from the posterior endpoint of SC to the TM bordering the ICA anterior to the scleral spur (TMH), and TM length as distance from scleral spur to Schwalbe line. *Bottom*: Iridocorneal angle measurements were acquired semiautomatically using the device software: angle opening distance at 500/750 µm from the apex of the scleral spur (AOD-500, -750), trabecular iris angle at 500/750 µm (TIA-500, -750), and trabecular iris space area at 500/750 µm (TISA-500, -750).

Participants

Inclusion criteria were as follows: age 4 to 16 years, healthy eyes (visual acuity normal for age, normal IOP). Participants' parents gave written informed consent; children could give written assent.

Between May 16, 2016 and September 12, 2016, we enrolled 50 children, which is a sample size commonly used in exploratory studies.

Demographic and Clinical Data

From the medical notes, we recorded age, ethnicity, refractive error when present (last refraction within 12 months prior to study visit), and whether refraction was performed with or without cycloplegia.

AS-OCT

We acquired high-resolution AS-OCT images of the nasal ICA of both eyes (Tomey SS-1000; CASIA, Nagoya, Japan). We used standard device settings, acquiring 64 horizontal raster B-scans and 512 A-scans of a rectangular area of 8×4 mm (1600×838 pixels), centered on the nasal limbus, over 1.2 seconds. All images were obtained in a dimmed room by the same observer (MD), following a standardized imaging protocol and specifying two levels of accommodation.

It was not possible to use the optical targets built into the device, as these can only be used in primary position of gaze. Our region of interest, the ICA, is best imaged in slight side gaze. Light emitting diodes (LEDs) are mounted onto the device casing, and we had planned to use these as near targets ("light"). However, some children could not fixate on the LED; we therefore used a handheld target next to the LED, at 6.5 cm from the eye, as an additional near target ("near object"). The accommodative effort induced was approximately 15 D.

In preliminary assessments, we noticed that a distance target at 3 m from the eye was for some children not sufficient to maintain interest for long enough to allow the acquisition of the OCT scans. We therefore again used a handheld target, held at 40 cm from the eye, for distance fixation. The accommodative effort induced was thus 2.5 D ("relaxed accommodation").

Measurements on AS-OCT Images

One observer (MD) carried out the analysis of all images. The difference in angle configuration between relaxed accommodation and accommodative effort prevented genuine masking. A second, independent observer (AHA) repeated SC measurements. To confirm that accommodative effort had been exerted with near fixation, we measured CM width at three locations; with accommodation, the anterior portion of the CM width is expected to increase.[27–29] We acquired triplicate measurements of the CM width at 1, 2, and 3 mm posterior to the scleral spur (CM-1, CM-2, CM-3) (Fig.).

The point at which optically dark CM changed to brighter TM was defined as the scleral spur; the Schwalbe line was defined as the border between bright corneal endothelium and darker TM; and the anteroposterior SC diameter (SC-APD) was measured as the anteroposterior extent of dark space external to the TM.

As SC is frequently tear shaped, with greatest height posteriorly, we measured its radial diameter (SC-RD) at three locations and calculated the average. We measured the cross-sectional area of SC (SC-CSA) by outlining the SC contour using the freehand tool and measuring the area of the resulting shape. Similarly, we measured trabecular meshwork area (TMA, defined as the area enclosed by a line connecting the scleral spur, posterior endpoint of SC, and Schwalbe's line), and trabecular meshwork length and height (TML and TMH, defined as the distance from the Schwalbe line to the inferoposterior edge of TM [TML], and as the distance from the posterior endpoint of SC to the TM bordering the ICA anterior to the scleral spur [TMH], respectively). To quantify TM density (TMD), we exported the raw images into FIJI (ImageJ version 2.0.0-rc-30/1.50b [http://imagej.net]; National Institutes of Health, Bethesda, MD, USA), outlined the TM area using the freehand tool, and analyzed the mean gray value.

ICA measurements were semiautomated: after marking of angle recess and the apex of the scleral spur, we noted angle opening distance at 500/750 µm from the apex of the scleral spur (AOD-500, -750), trabecular iris angle at 500/750 µm (TIA-500, -750), and trabecular iris space area at 500/750 µm (TISA-500, -750).[30] All measurements were carried out in triplicate, and the mean of three measurements was used for further analysis.

Statistical Analysis

MD entered data onto a spreadsheet in Excel (Microsoft, Redmond, WA, USA). We calculated the means of triplicate image measurements. We included all available unilateral and bilateral data from all participants in the analysis.

Descriptive statistics are presented as mean and SD for continuous approximately normally distributed data and median and interquartile range for continuous non-normally distributed data (normality assessed using quantile-quantile

Table 1. Demographic and Refractive Participant Characteristics

Characteristic	*n* (%)	Summary Statistics
Age, y, mean (SD)	50 (100%)	10.9 (3.0)
Female	29 (58%)	
Ethnic group		
White	8 (16%)	
Asian/Asian British	8 (16%)	
Black/black British	4 (8%)	
Mixed	11 (22%)	
Other	3 (6%)	
Unknown	16 (32%)	
SE, D, median (IQR)	41 (82%)	
Right eye		0.25 (−0.13, 0.88)
Left eye		0 (−0.13, 0.75)

IQR, interquartile range.

plots). Categorical data are presented as frequencies and percentages.

Three level random effects models were used to estimate the average difference between levels of accommodation with respective 95% confidence interval (CI) for each parameter (5% significance level). This method allows accounting for correlation between measurements taken from the same participant (repeated measurements within eye and eyes nested within participants). A random coefficient for state of accommodation was used for the cases where there was evidence of model fit improvement compared with a fixed coefficient.

Data not approximately normally distributed were log-transformed, and analysis was conducted on the transformed data. Missing data were not imputed, and therefore analysis was conducted on available data. Analysis was conducted in Stata/MP version 14 (StataCorp LLC, College Station, TX, USA). To investigate the role of age and refractive error, we conducted exploratory analyses by fitting the main analysis models while adding age and refractive error as covariates separately. We fit both covariates together only when each covariate was statistically significant and we had more than 30 observations to fit the model.

Results

Participants

We enrolled 50 children and young people and imaged both eyes in all participants. Table 1 summarizes demographic and refractive characteristics.

Confirmation of Accommodative Effort

Data were available on 71 eyes from 37 patients for ciliary muscle width at 1 mm posterior to the scleral spur (CM1). There was a statistically significant increase by 0.025 mm (95% CI: 0.01, 0.04), or 5%, between intense near accommodative effort and relaxed accommodation: with relaxed accommodation, CM1 measured 0.658 mm (95% CI: 0.628, 0.689), and with accommodative effort, CM1 measured 0.680 mm (95% CI: 0.650, 0.710).

Changes in SC, TM, and ICA During Accommodation

SC measurements by two observers showed good agreement (data not shown). With accommodative effort, radial and anteroposterior SC diameter and SC-CSA increased significantly (Table 2). Except for an increase in length with accommodation, we did not detect a significant change in TM parameters.

All conventional ICA parameters (i.e., angle opening distance, trabecular iris angle, and trabecular iris space area) increased significantly with intense accommodative effort; only the increase in TISA at 500 μm anterior to the scleral spur did not reach statistical significance (Table 2).

Association Between Age/Refractive Effort and Accommodation-Induced Changes on the Random Fit Model

For SC anteroposterior diameter and CSA, there was a statistically significant association with age: if accommodative state is held constant, the anteroposterior diameter decreased by 0.012 mm (95% CI: 0.005, 0.019) per year increase in age, and logarithmic CSA decreased by 0.08 mm (95% CI: 0.019, 0.133) per year increase in age.

For trabecular iris angles 500 and 700 μm, there was a statistically significant association with spherical equivalent (SE): if state is held constant, TIA_{500} decreased by 2.10° (95% CI: 0.51, 5.48) and TIA_{750} decreased by 2.87° (95% CI: 0.98, 4.77) per diopter increase in SE. Similar results were observed for trabecular iris space area $(TISA)_{750}$: a decrease of 0.04 mm^2 (95% CI: 0.008, 0.072) per diopter increase in SE, but not for $TISA_{500}$, where there was no evidence of an association with SE.

Discussion

Key Findings

This is, to our knowledge, the first study to demonstrate morphologic changes in aqueous outflow structures during accommodation in humans, reporting an increase in anteroposterior and radial diameter and CSA of SC and in the length of the TM during accommodative effort. It bridges the gap between studies that have shown an increase in SC CSA following CM contraction induced by pilocarpine or electrical stimulation of the Edinger-Westphal nucleus,[16–21,31] and OCT imaging studies of the aqueous outflow structures.[22,23,26] In addition, this study reports a reduction in SC size with increasing age. A third finding, to our knowledge not previously reported in healthy children, is that, in eyes with greater SE (hypermetropia), the iridicorneal angle is narrower.

Limitations

Although our use of nonvalidated accommodative targets and lack of formal monitoring of accommodation during OCT acquisition using an autorefractor may be considered a limitation of our study, the increase in the anterior portion of the ciliary muscle we used as a proxy of accommodative effort has previously been shown to correlate with accommodation.[27–29] Similar to previous reports, we also observed a significant thinning of the posterior portion of CM with accommodation.[28,29] We therefore consider our approach to be a valid method to confirm accommodative effort, although future studies may include autorefractor monitoring of accommodation. Image quantification by a nonmasked observer is a limitation that should also be addressed in future work.

Our acquisition of OCT images in one nasal location is a limitation of our study: SC diameter is now known to vary considerably along the limbal circumference.[32,33] This may at least in part explain why complete image sets allowing quantification of the aqueous outflow structures with different levels of accommodation could only be acquired in approxi-

Table 2. SC Dimensions and CSA Significantly Increase During Intense Accommodative Effort

Structure	Relaxed Accommodation				Intense Near Accommodative Effort				Difference			95% CI for Difference		Significance (Two-Tailed)
	N	Right Eye, Mean (SD)	*N*	Left Eye, Mean (SD)	*N*	Right Eye, Mean (SD)	*N*	Left Eye, Mean (SD)	*N* Eyes		Mean (SE)	Lower	Upper	
SC														
Radial diameter (mm)	24	0.014 (0.006)	25	0.017 (0.006)	22	0.027 (0.014)	25	0.027 (0.011)	37	67	0.011 (0.001)	0.008	0.014	**<0.001**
Anteroposterior diameter (mm)	24	0.184 (0.088)	24	0.241 (0.103)	21	0.297 (0.089)	26	0.250 (0.109)	36	66	0.060 (0.019)	0.023	0.097	**0.002**
CSA (mm^2)*	24	−5.46 (0.958)	24	−4.83 (0.854)	21	−4.49 (0.697)	26	−4.75 (0.829)	36	66	0.507 (0.175)	0.165	0.849	**0.004**
CSA (mm^2)†	24	0.0043	24	0.0080	21	0.0112	26	0.0087						
TM														
Area (mm^2)	27	0.080 (0.028)	22	0.073 (0.019)	31	0.078 (0.017)	27	0.075 (0.022)	36	66	−0.001 (0.003)	−0.007	0.005	0.743
Height (mm)	30	0.282 (0.042)	33	0.282 (0.050)	33	0.267 (0.040)	30	0.278 (0.048)	35	70	−0.010 (0.007)	−0.023	0.003	0.14
Length (mm)	22	0.436 (0.084)	32	0.401 (0.075)	31	0.453 (0.073)	28	0.444 (0.073)	34	66	0.030 (0.009)	0.011	0.048	**0.002**
Density (units)	29	114.54 (27.64)	33	113.09 (19.95)	33	114.82 (18.65)	29	119.22 (18.86)	35	69	3.657 (2.635)	−1.508	8.822	0.165
Angle opening distance														
500 μm anterior to scleral spur (mm)	2	0.740 (0.083)	19	0.616 (0.206)	2	0.854 (0.495)	29	0.735 (0.279)	35	36	0.147 (0.044)	0.06	0.234	**0.001**
750 μm anterior to scleral spur (mm)	4	1.084 (0.311)	20	0.820 (0.241)	2	1.152 (0.468)	30	0.974 (0.299)	37	39	0.159 (0.043)	0.074	0.243	**<0.001**
Trabecular iris angle														
500 μm anterior to scleral spur (°)	2	62.3 (13.53)	14	44.55 (11.11)	2	45.22 (16.76)	29	49.11 (11.10)	32	33	5.298 (1.778)	1.814	8.782	**0.003**
750 μm anterior to scleral spur (°) (mm^2)	2	59.67 (8.72)	16	45.79 (8.88)	2	49.15 (12.70)	30	49.69 (9.68)	33	34	5.64 (1.57)	2.556	8.73	**<0.001**
Trabecular iris space area														
500 μm anterior to scleral spur (mm^2)	4	0.273 (0.068)	20	0.226 (0.102)	2	0.272 (0.153)	30	0.243 (0.104)	36	38	0.015 (0.020)	−0.024	0.055	0.45
750 μm anterior to scleral spur (mm^2)	2	0.576 (0.089)	17	0.409 (0.135)	2	0.513 (0.251)	30	0.468 (0.173)	33	34	0.067 (0.029)	0.009	0.124	**0.024**

$P < 0.05$ values are in bold.

* Highly skewed distribution and therefore the results presented here are from log-transforming the data.

† Original mean in mm^2.

mately 30% of our participants. Other authors report higher visualization rates, using multiple scans[32] or averaging of several scans.[34] Working with children, we opted to use the standard settings to keep scanning time as short as possible.

We used a nonvalidated target to induce intense accommodative effort but observed a 5% increase in anterior CM thickness, which is similar to the increase observed in studies that controlled levels of accommodation.[27–29]

External Validity of Findings

Our manual measurements of SC and TM dimensions are similar in magnitude to those previously reported (i.e., anteroposterior SC diameter in the range of 0.2 to 0.3 mm,[34,35] radial diameter in the range of 0.015 to 0.03 mm, and TM area around 0.08),[34,35] confirming the validity of our measurements. Similar to pilocarpine studies,[17,31] we observed an increase in SC CSA during physiologic accommodation.

With accommodative effort, we observed an increase in TM length but not height; an OCT study in mice using pilocarpine to induce CM contraction equally reported no change in TM height.[17] It has been suggested that CM contraction pulls the TM lamellae toward the center of the eye, leading to an expansion of the spaces between the TM lamellae,[15,19] but imaging studies providing evidence for this process are lacking, both with OCT and histology.[17,36] It is possible that rather than an expansion of TM spaces or total TM height, CM contraction may induce a change in the configuration of the meshwork, allowing increased outflow of aqueous toward SC. It is also possible that the age-related decrease in SC dimensions does not reflect true change, but merely that the diameter falls below the limit imposed by image resolution. In vivo imaging using second harmonic generation technology[14] may offer higher resolution visualization of the TM in an intact eye.

Although limited by our lack of IOP data in this cohort, our findings may contribute to an understanding of IOP regulation in healthy human eyes. IOP in children is known to be lower than in adults,[1–5] and higher amplitude of accommodation may play a role in the promotion of aqueous outflow. Static and repeated accommodation significantly reduces IOP in young adults,[13] although others report that IOP may rise during accommodation in adults[37] and in progressing myopes.[38] SC dimensions correlate with outflow facility[39] and have an effect on outflow resistance.[40,41] The inner wall of SC and the juxtacanalicular portion of the trabecular meshwork, which account for the majority of outflow resistance,[21,42] also respond to changes in mechanical tension.[43] Conversely, SC dimensions are reduced in eyes with high IOP.[17,33,44,45] Although we did not measure IOP or outflow facility, these previous studies indicate a link between morphology and function of aqueous outflow structures.

Our finding that the angle opening distance and trabecular iris angle increase during accommodation is novel. Only two previous studies used OCT to evaluate SC changes induced by pilocarpine.[17,31] Of these two, one explored SC in humans, but did not evaluate changes in ICA parameters used in glaucoma patients.[31] The other reported that, in mice, the angle between cornea and iris did not change[17]; this parameter is slightly different from TIA, and differences in angle morphology between rodents and humans may contribute to this finding, which is in conflict with our report.

In summary, this study demonstrates the effect of physiologic accommodation in humans on the morphology of structures of the aqueous outflow, indicating that accommodation may contribute to IOP regulation in children and young adults. High-resolution OCT can be used to visualize dynamic morphologic changes in outflow structures not only after pharmacologic stimulation[31] or glaucoma surgery,[35] but also with physiologic accommodation.

Acknowledgments

The authors thank Marie Restori for advice and support on acquiring anterior segment OCT images and Eme Chan and Konstantina Prapa for help with approaching families about taking part in this study. We thank the children who took part in this study and their families who selflessly gave their time to help other children in the future. The views expressed are those of the authors and not necessarily those of the National Health Service, the NIHR, or the Department of Health.

Supported by the National Institute for Health Research (NIHR) Moorfields Biomedical Research Centre and funded by The Wates Foundation, Fight for Sight (Small Grant Award 1706/07), and Moorfields Eye Charity.

Disclosure: **M.C. Daniel**, None; **A.M. Dubis**, None; **A. Quartilho**, None; **H. Al-Hayouti**, None; **Sir P.T. Khaw**, None; **M. Theodorou**, None; **A. Dahlmann-Noor**, None

References

1. Goethals M, Missotten L. Intraocular pressure in children up to five years of age. *J Pediat Ophthalmol Strabismus*. 1983; 20:49–51.
2. Pensiero S, Da Pozzo S, Perissutti P, Cavallini GM, Guerra R. Normal intraocular pressure in children. *J Pediat Ophthalmol Strabismus*. 1992;29:79–84.
3. Sihota R, Tuli D, Dada T, Gupta V, Sachdeva MM. Distribution and determinants of intraocular pressure in a normal pediatric population. *J Pediat Ophthalmol Strabismus*. 2006;43:14–18.
4. Dusek WA, Pierscionek BK, McClelland JF. Age variations in intraocular pressure in a cohort of healthy Austrian school children. *Eye*. 2012;26:841–845.
5. Jaafar MS, Kazi GA. Normal intraocular pressure in children: a comparative study of the Perkins applanation tonometer and the pneumatonometer. *J Pediat Ophthalmol Strabismus*. 1993;30:284–287.
6. Chattopadhyay DN, Seal GN. Amplitude of accommodation in different age groups and age of on set of presbyopia in Bengalee population. *Ind J Ophthalmol*. 1984;32:85–87.
7. Jimenez R, Gonzalez MD, Perez MA, Garcia JA. Evolution of accommodative function and development of ocular movements in children. *Ophthalmic Physiologic Optics*. 2003;23: 97–107.
8. Sterner B, Gellerstedt M, Sjostrom A. The amplitude of accommodation in 6-10-year-old children: not as good as expected! *Ophthalmic Physiologic Optics*. 2004;24:246–251.
9. Benzoni JA, Rosenfield M. Clinical amplitude of accommodation in children between 5 and 10 years of age. *Optom Vis Dev*. 2012;43:109–114.
10. Ovenseri-Ogbomo GO, Kudjawu EP, Kio FE, Abu EK. Investigation of amplitude of accommodation among Ghanaian school children. *Clin Exp Optom*. 2012;95:187–191.
11. Castagno VD, Vilela MA, Meucci RD, et al. Amplitude of accommodation in schoolchildren. *Curr Eye Res*. 2016;42:1–7.
12. Hashemi H, Nabovati P, Yekta AA, et al. Amplitude of accommodation in an 11- to 17-year-old Iranian population. *Clin Exp Optom*. 2017;100:162–166.
13. Jenssen F, Krohn J. Effects of static accommodation versus repeated accommodation on intraocular pressure. *J Glaucoma*. 2012;21:45–48.
14. Park CY, Lee JK, Kahook MY, Schultz JS, Zhang C, Chuck RS. Revisiting ciliary muscle tendons and their connections with the trabecular meshwork by two photon excitation micro-

scopic imaging. *Invest Ophthalmol Vis Sci*. 2016;57:1096–1105.

15. Rohen JW, Lutjen E, Barany E. The relation between the ciliary muscle and the trabecular meshwork and its importance for the effect of miotics on aqueous outflow resistance. A study in two contrasting monkey species, *Macaca irus* and *Cercopithecus aethiops*. *Albrecht Von Graefes Arch Klin Exp Ophthalmol*. 1967;172:23–47.
16. Barany EH. The mode of action of miotics on outflow resistance. A study of pilocarpine in the vervet monkey *Cercopithecus ethiops*. *Trans Ophthalmol Soc UK*. 1966;86:539–578.
17. Li G, Farsiu S, Chiu SJ, et al. Pilocarpine-induced dilation of Schlemm's canal and prevention of lumen collapse at elevated intraocular pressures in living mice visualized by OCT. *Invest Ophthalmol Vis Sci*. 2014;55:3737–3746.
18. Tektas OY, Lutjen-Drecoll E. Structural changes of the trabecular meshwork in different kinds of glaucoma. *Exp Eye Res*. 2009;88:769–775.
19. Lutjen-Drecoll E. Structural factors influencing outflow facility and its changeability under drugs. A study in *Macaca arctoides*. *Invest Ophthalmol*. 1973;12:280–294.
20. Lutjen-Drecoll E. Functional morphology of the trabecular meshwork in primate eyes. *Progr Retinal Eye Res*. 1999;18:91–119.
21. Roy Chowdhury U, Hann CR, Stamer WD, Fautsch MP. Aqueous humor outflow: dynamics and disease. *Invest Ophthalmol Vis Sci*. 2015;56:2993–3003.
22. Kuchem MK, Sinnott LT, Kao CY, Bailey MD. Ciliary muscle thickness in anisometropia. *Optom Vis. Sci*. 2013;90:1312–1320.
23. Goel M, Picciani RG, Lee RK, Bhattacharya SK. Aqueous humor dynamics: a review. *Open Ophthalmol J*. 2010;4:52–59.
24. Sun FC, Stark L, Nguyen A, Wong J, Lakshminarayanan V, Mueller E. Changes in accommodation with age: static and dynamic. *Am J Optom Physiol Opt*. 1988;65:492–498.
25. Atchison DA, Capper EJ, McCabe KL. Critical subjective measurement of amplitude of accommodation. *Optom Vis Sci*. 1994;71:699–706.
26. Liu S, Yu M, Ye C, Lam DS, Leung CK. Anterior chamber angle imaging with swept-source optical coherence tomography: an investigation on variability of angle measurement. *Invest Ophthalmol Vis Sci*. 2011;52:8598–8603.
27. Sheppard AL, Davies LN. In vivo analysis of ciliary muscle morphologic changes with accommodation and axial ametropia. *Invest Ophthalmol Vis Sci*. 2010;51:6882–6889.
28. Lossing LA, Sinnott LT, Kao CY, Richdale K, Bailey MD. Measuring changes in ciliary muscle thickness with accommodation in young adults. *Optom Vis Sci*. 2012;89:719–726.
29. Lewis HA, Kao CY, Sinnott LT, Bailey MD. Changes in ciliary muscle thickness during accommodation in children. *Optom Vis Sci*. 2012;89:727–737.
30. Leung CK, Li H, Weinreb RN, et al. Anterior chamber angle measurement with anterior segment optical coherence tomography: a comparison between slit lamp OCT and Visante OCT. *Invest Ophthalmol Vis Sci*. 2008;49:3469–3474.
31. Skaat A, Rosman MS, Chien JL, et al. Effect of pilocarpine hydrochloride on the Schlemm canal in healthy eyes and eyes with open-angle glaucoma. *JAMA Ophthalmol*. 2016;134:976–981.
32. Kagemann L, Nevins JE, Jan NJ, et al. Characterisation of Schlemm's canal cross-sectional area. *Br J Ophthalmol*. 2014;98(suppl 2):ii10–ii14.
33. Hann CR, Vercnocke AJ, Bentley MD, Jorgensen SM, Fautsch MP. Anatomic changes in Schlemm's canal and collector channels in normal and primary open-angle glaucoma eyes using low and high perfusion pressures. *Invest Ophthalmol Vis Sci*. 2014;55:5834–5841.
34. Usui T, Tomidokoro A, Mishima K, et al. Identification of Schlemm's canal and its surrounding tissues by anterior segment fourier domain optical coherence tomography. *Invest Ophthalmol Vis Sci*. 2011;52:6934–6939.
35. Fuest M, Kuerten D, Koch E, et al. Evaluation of early anatomical changes following canaloplasty with anterior segment spectral-domain optical coherence tomography and ultrasound biomicroscopy. *Acta Ophthalmol*. 2016;94:e287–e292.
36. Overby DR, Bertrand J, Schicht M, Paulsen F, Stamer WD, Lutjen-Drecoll E. The structure of the trabecular meshwork, its connections to the ciliary muscle, and the effect of pilocarpine on outflow facility in mice. *Invest Ophthalmol Vis Sci*. 2014;55:3727–3736.
37. Liu Y, Lv H, Jiang X, Hu X, Zhang M, Li X. Intraocular pressure changes during accommodation in progressing myopes, stable myopes and emmetropes. *PLoS One*. 2015;10:e0141839.
38. Yan L, Huibin L, Xuemin L. Accommodation-induced intraocular pressure changes in progressing myopes and emmetropes. *Eye (Lond)*. 2014;28:1334–1340.
39. Chen J, Huang H, Zhang S, Chen X, Sun X. Expansion of Schlemm's canal by travoprost in healthy subjects determined by Fourier-domain optical coherence tomography. *Invest Ophthalmol Vis Sci*. 2013;54:1127–1134.
40. Moses RA, Hoover GS, Oostwouder PH. Blood reflux in Schlemm's canal. I. Normal findings. *Arch Ophthalmol*. 1979;97:1307–1310.
41. Moses RA. Circumferential flow in Schlemm's canal. *Am J Ophthalmol*. 1979;88:585–591.
42. Johnson M. What controls aqueous humour outflow resistance? *Exp Eye Res*. 2006;82:545–557.
43. Braakman ST, Read AT, Chan DW, Ethier CR, Overby DR. Colocalization of outflow segmentation and pores along the inner wall of Schlemm's canal. *Exp Eye Res*. 2015;130:87–96.
44. Allingham RR, de Kater AW, Ethier CR. Schlemm's canal and primary open angle glaucoma: correlation between Schlemm's canal dimensions and outflow facility. *Exp Eye Res*. 1996;62:101–109.
45. Hong J, Xu J, Wei A, et al. Spectral-domain optical coherence tomographic assessment of Schlemm's canal in Chinese subjects with primary open-angle glaucoma. *Ophthalmology*. 2013;120:709–715.

Investigative Ophthalmology & Visual Science